

# The Hot White Dwarf in the Cataclysmic Variable MV Lyrae<sup>1</sup>

D. W. Hoard

*SIRTF Science Center, California Institute of Technology, Mail Code 220-6, 1200 E. California Blvd., Pasadena CA 91125*  
hoard@ipac.caltech.edu

A. P. Linnell<sup>2</sup>

*Department of Physics and Astronomy, Michigan State University, East Lansing, MI 48824*  
linnell@astro.washington.edu

Paula Szkody

*Department of Astronomy, University of Washington, Box 351580, Seattle WA 98195-1580*  
szkody@astro.washington.edu

Robert E. Fried

*Braeside Observatory, P. O. Box 906, Flagstaff AZ 86002*  
captain@asu.edu

Edward M. Sion

*Department of Astronomy and Astrophysics, Villanova University, Villanova, PA 19085;*  
edward.sion@villanova.edu

Ivan Hubeny

*Laboratory for Astronomy and Solar Physics, NASA Goddard Space Flight Center, Code 681, Greenbelt MD 20771*  
hubeny@tlusty.gsfc.nasa.gov

M. A. Wolfe

*Department of Astronomy, University of Washington, Box 351580, Seattle WA 98195-1580*  
maw2323@u.washington.edu

## ABSTRACT

We have obtained the first far-ultraviolet spectrum of the novalike cataclysmic variable MV Lyrae using the *Far Ultraviolet Spectroscopic Explorer*. We also obtained contemporaneous optical light curves and spectra. All data are from a deep faint accretion state of MV Lyr. We constructed a model for the system using the BINSYN software package; results from this model include the following: (1) The white dwarf has  $T_{\text{eff}} = 47,000$  K, photospheric  $\log g = 8.25$ , and metallicity of  $Z = 0.3Z_{\odot}$ . (2) The secondary star is cooler than 3500 K; it contributes nothing to the far-ultraviolet

---

<sup>2</sup>Visiting Scholar, University of Washington.

flux and a varying amount to the optical flux (from 10% at 5200 Å to 60% at 7800 Å). (3) The accretion disk, if present at all, contributes negligibly to the spectrum of MV Lyr. Irradiation considerations imply that the mass transfer rate is no more than  $3 \times 10^{-13} M_{\odot} \text{ yr}^{-1}$ . (4) Assuming no disk is present, the model optical light curve has an amplitude approximately 50% larger than that of the sinusoidal modulation (on the orbital period) in the observed optical light curve, suggesting that the secondary star might be shaded by a nascent disk and/or be slightly detached from its Roche lobe. (5) The scaling of the model spectrum to the observed data leads to a distance of  $d = 505 \pm 50 \text{ pc}$  to MV Lyr.

*Subject headings:* accretion, accretion disks — novae, cataclysmic variables — stars: individual (MV Lyrae) — ultraviolet: stars — white dwarfs

## 1. Introduction

Cataclysmic variables (CVs) are semi-detached binary stars in which a late main sequence star loses mass onto a white dwarf (WD) via Roche lobe overflow. In systems containing a non-magnetic WD, accretion proceeds through a viscous disk. CVs are often classified into groups based on their photometric properties and outburst behavior. Unlike the more well-known dwarf nova class of CV, members of the novalike class do not undergo quasiperiodic outbursts. Novalikes are instead characterized by an approximately steady, high rate of mass transfer (and correspondingly luminous accretion disk) that quenches the disk instability mechanism responsible for dwarf nova outbursts. Although the mass transfer process in novalike CVs is (on average) steady, some novalikes (the so-called VY Sculptoris stars) occasionally undergo faint states in which mass transfer is severely reduced or shut off completely. When this happens, the accretion disk decreases in size or disappears completely, and the overall system brightness fades by several magnitudes. During the faint state, the component stars are clearly viewed and the system parameters (stellar masses and temperatures, etc.) can be best determined. See Warner (1995) for a thorough review of CV types and behavior.

MV Lyrae is a novalike CV of the VY Scl subclass. It is normally found at a brightness of  $V \approx 12\text{--}13$ , but undergoes faint states during which it drops to  $V \approx 16\text{--}18$ . A long-term optical light curve of MV Lyr, compiled over the last 5 years by contributors to the American Association of Variable Star Observers (AAVSO) is shown in Figure 1 (Mattei, J. A., 2003, Observations from the AAVSO International Database, private communication). The bright and faint states characteristic of VY Scl stars are apparent in the light curve. Schneider, Young, & Sackett (1981, henceforth,

---

<sup>1</sup>This research is based on observations with the NASA-CNES-CSA *Far Ultraviolet Spectroscopic Explorer*, which is operated for NASA by the Johns Hopkins University under NASA contract NAS 5-32985, and on observations obtained with the Apache Point Observatory 3.5-meter telescope, which is owned and operated by the Astrophysical Research Consortium.

SYS81) reported a spectroscopic orbital period of 0.1336(17) d ( $\approx 3.21$  hr) measured during a faint state of MV Lyr. This orbital period was later refined to  $P_{\text{orb}} = 0.1329(4)$  d ( $\approx 3.19$  hr) by Skillman, Patterson, & Thorstensen (1995, henceforth, SPT95), who performed a photometric and spectroscopic observing campaign on MV Lyr in its bright state during 1993. Additional quasi-periodic photometric periods of approximately 48 minutes and 3.6 days, although reasonably well-established by SPT95 (and references therein), have not yet been fully explained (the longer period may be the apsidal precession period of the disk). The combination of low and high state spectroscopic data obtained by SYS81 and SPT95 established  $K$  velocity amplitudes for both the WD and secondary star, yielding a mass ratio of  $q (= M_2/M_{\text{wd}}) \sim 0.4$ . The lack of eclipses and small radial velocity amplitudes in MV Lyr suggest an inclination of  $i = 10\text{--}13^\circ$  (SYS81, SPT95).

Faint state spectra of MV Lyr from the *International Ultraviolet Explorer* (*IUE*) satellite (discussed in Section 3.3) gave indications of a hot ( $T \sim 50,000$  K) WD in this system (Chiappetti et al. 1982; Szkody & Downes 1982). Because CVs in the orbital period range  $P_{\text{orb}} = 3\text{--}4$  hr typically have high time-averaged accretion rates, it is especially important to study them during faint states when the luminosity contribution from the accretion disk is negligible. In addition to offering a clear view of the stellar components, this condition allows us to study the effects of heating of the WD during prolonged periods of accretion (and its subsequent cooling in the absence of accretion). Thus, we utilized the unique capabilities of the *Far Ultraviolet Spectroscopic Explorer* (*FUSE*), together with ground-based optical observations, to study the properties of MV Lyr in the midst of a recent faint state that lasted approximately 8 months (see Figure 1). These observations have provided us with a detailed look at the hot WD in this CV, and allowed us to make conclusive estimates of the WD’s physical properties (e.g., temperature, mass, chemical composition, etc.), as well as systemic parameters such as distance and faint state mass transfer rate.

## 2. Observations

### 2.1. Optical Photometry

We obtained time series photometry of MV Lyr on HJD 2452462.67–.90 (2002 July 07) and HJD 2452463.67–0.95 (2002 July 08). These data bracket the time of our *FUSE* observation of MV Lyr (see Section 2.3). The CCD observations were made in unfiltered light at Braeside Observatory<sup>3</sup> with a time resolution of  $\approx 190$  s per measurement. Bad weather and hardware problems plagued the first night of observations, but the data from the second night are optimal. Differential light curves for the two nights are shown in Figure 2. The comparison star used to construct the differential light curves has  $V = 14.70$  (Henden & Honeycutt 1995). Compared to the mean unfiltered differential magnitude from July 08, this allows us to estimate the mean brightness of MV Lyr during our photometric (and *FUSE*) observations as  $V \approx 17.8$ . This is near the most faint

---

<sup>3</sup>See <http://braeside.la.asu.edu/> for observatory and instrument details.

extreme ( $V \approx 18$ ) of MV Lyr’s faint accretion states (see Figure 1).

We used power spectrum analysis (both with and without application of the CLEAN algorithm; Roberts, Lehár, & Dreher 1987) and sine wave fitting (using custom IDL code) to search for periodicities in our time series photometry. Because of the aforementioned problems with the July 07 data, we performed the period searches using only the higher quality July 08 data. The only periodic variability we found is consistent with the known orbital period of MV Lyr:  $P_{\text{orb}} = 0.1329(4)$  d (SPT95),  $P_{\text{power}} = 0.135(45)$  d, and  $P_{\text{sine}} = 0.1330(19)$  d. The solid curve in Figure 2 shows the best-fitting sine function. The dotted curve in the top panel of the figure (the July 07 light curve) has been offset by the difference between the mean magnitude of each data set. It is not clear if the 0.03 mag difference in the mean magnitude between the two nights represents a real change in the mean brightness of MV Lyr, or is just an artifact of the poor data quality on July 07.

## 2.2. Optical Spectroscopy

We obtained contemporaneous optical spectra of MV Lyr on HJD 2452458.89 (2002 July 03, 09:09–09:34 UT), using the Double Imaging Spectrograph (DIS) on the 3.5-m telescope at Apache Point Observatory<sup>4</sup> (APO). Two 10-minute exposures were obtained, each covering wavelength ranges of 3800–5400 Å on the blue side of DIS and 5960–7900 Å on the red side of DIS. The blue and red spectra have dispersions of  $\approx 1.6$  Å pixel<sup>-1</sup> and  $\approx 1.1$  Å pixel<sup>-1</sup>, respectively. Intermittent clouds were present during the observations, so the absolute flux level is not reliable. Figure 3 shows the better of the two pairs of red and blue spectra. Weak absorption troughs are visible around the Balmer lines, and He II  $\lambda 4686$  appears to be present solely as a weak absorption feature. Overall, our spectra are similar in appearance to the faint state optical spectra of MV Lyr obtained by SYS81 and Szkody & Downes (1982).

## 2.3. Far-ultraviolet Spectroscopy

We observed MV Lyr with *FUSE* during 4 exposures on HJD 2452463 (2002 July 07, 11:57–17:23 UT; see Table 1). All data were obtained using the LWRS aperture and TTAG accumulation mode (for *FUSE* spacecraft and instrument details see, for example, Sahnou et al. 2000<sup>5</sup>). We used the CalFuse v2.4.0 pipeline software to extract the FUV spectra from the raw data files obtained during each *FUSE* exposure. This version of the pipeline includes a module to correct for spacecraft “jitter” inherent to the new attitude control system, which was successfully implemented following the failure of two reaction wheels in late 2001. We then used a custom-built IDL routine (following

---

<sup>4</sup>See <http://www.apo.nmsu.edu/> for observatory and instrument details.

<sup>5</sup>Also see the *FUSE* Science Center web page at <http://fuse.pha.jhu.edu/>.

the recipes in the *FUSE* Data Analysis Cookbook<sup>6</sup>) to combine the various detector and mirror segments of the spectra. This yields a time-averaged spectrum with a total equivalent exposure time of  $\approx 11$  kiloseconds. We excluded the LiF1b data ( $\lambda = 1095\text{--}1187$  Å) in order to avoid the artifact known as “The Worm” (only the LiF2a data in this region are used). The final combined spectrum (see Figure 4) was rebinned onto a uniform wavelength scale with dispersion  $0.10$  Å pixel<sup>-1</sup> by averaging flux points from the original dispersion ( $0.007$  Å pixel<sup>-1</sup>) into wavelength bins of width  $0.10$  Å.

The time-averaged *FUSE* spectrum of MV Lyr has a mean continuum level of  $F_\lambda \approx 5\text{--}7 \times 10^{-14}$  erg s<sup>-1</sup> cm<sup>-2</sup> Å<sup>-1</sup> at wavelengths longer than  $1000$  Å. Shortward of  $1000$  Å, the continuum level decreases approximately monotonically to  $F_\lambda \approx 2 \times 10^{-14}$  erg s<sup>-1</sup> cm<sup>-2</sup> Å<sup>-1</sup> at  $\lambda = 920$  Å. Since the AAVSO light curve shows that MV Lyr was in a deep faint state (see Figure 1), it is not surprising that the *FUSE* spectrum is dominated by broad absorption lines corresponding to the photospheric features of a naked WD. In addition, a number of narrow interstellar absorption lines of various metal ions are visible in the spectrum.

In Table 2, we have listed the equivalent widths (EWs) for several WD photospheric absorption lines in the FUV spectrum of MV Lyr (measured by direct integration of pixel values between manually selected continuum points using the “e” routine in the IRAF<sup>7</sup> task SPLIT). The EWs are generally reproducible to within 10%. Although these lines were selected to be comparatively isolated and/or resolved multiplet members, the presence of superimposed interstellar and/or air-glow features makes the precise values of our directly measured EWs somewhat uncertain. For comparison, we have also provided the results of Gaussian fits to the line profiles (using the “k” routine in SPLIT) for some lines. Table 3 provides the EWs for interstellar absorption lines in the spectrum of MV Lyr, measured using only the “e” routine in SPLIT.

### 3. Analysis and Discussion

#### 3.1. WD-only Model Spectrum for the FUV Data

The past *IUE* observations of MV Lyr in faint states indicated the presence of a fairly hot WD (see Section 3.3). We first performed a number of initial comparisons of the *FUSE* spectrum with hot WD synthetic spectra, for a range of  $T_{\text{eff}}$  values, to locate a rough value for the WD  $T_{\text{eff}}$ . We then calculated a grid of NLTE WD model atmospheres with the program TLUSTY (v200) (Hubeny 1988; Hubeny & Lanz 1995), covering the  $T_{\text{eff}}$  range  $41,000\text{--}51,000$  K in steps of  $1000$  K, and the  $\log g$  range  $7.50\text{--}8.75$  in steps of  $0.25$ . The model atmospheres have compositions of 90%

---

<sup>6</sup>See <http://fuse.pha.jhu.edu/analysis/cookbook.html>.

<sup>7</sup>The Image Reduction and Analysis Facility is distributed by the National Optical Astronomy Observatory, which is operated by the Association of Universities for Research in Astronomy, Inc., under cooperative agreement with the National Science Foundation.

H and 10% He. We then used SYNSPEC (v45) (Hubeny, Stefl, & Harmanec 1985)<sup>8</sup> to calculate a synthetic spectrum for each model atmosphere. These spectra cover the wavelength range 800–1300 Å and have maximum spacing of 0.05 Å between tabulated wavelengths. Solar composition was assumed for the synthetic spectra during our initial analysis. The *FUSE* spectrum of MV Lyr was prepared for comparison to these synthetic WD template spectra by binning the *FUSE* data to a dispersion of 0.5 Å pixel<sup>-1</sup> and masking off the narrow geocoronal emission features. The synthetic spectra were convolved with a 1.0 Å broadening function prior to the fitting process.

Fitting a synthetic spectrum to our *FUSE* spectrum involves finding the optimum scaling factor to superpose the former on the latter. In order to judge the quality of the fit, we tested the following criteria: (1) the mean residual,  $\bar{r}_i$ , (2) the mean absolute residual,  $|\bar{r}_i|$ , (3) the standard deviation of the residuals,  $\sigma_r$ , (4) chi-squared,  $\chi^2$ , and (5) reduced chi-squared,  $\tilde{\chi}^2$ . For each candidate synthetic spectrum, we tabulated these statistics for a range of scaling factors. The minima of the statistics, as a function of scaling factor, determine the optimum scaling factor for a given synthetic spectrum. The relative minimum values of the statistics determine the overall best-fitting synthetic spectrum. Our tests show agreement among statistics (1), (2), (4), and (5). Statistic (3) had a minimum value near, but differing from, the consensus optimum scaling factor. All of the statistics varied smoothly through the tabulation range of the scaling factor. We do not present scaling factor results for our initial/intermediate model spectrum fits; instead, the scaling factor results for our final, full-system model are presented and discussed in Section 3.2. In all cases, the method described here was used to determine the optimum scaling factor. Our initial, WD-only fit resulted in WD parameters of  $T_{\text{eff}} = 47,000$  K and  $\log g = 8.25$ .

We next considered the effect of non-solar atmospheric composition of the WD. We calculated a new set of synthetic spectra at a resolution of 0.05 Å, using the H-He model atmosphere from TLUSTY (v200) with the best-fit parameters from our initial fitting, for metallicities of  $Z = 0.1$ – $1.0Z_{\odot}$  in steps of  $0.1Z_{\odot}$  (where the coefficient of  $Z_{\odot}$  is a factor multiplying the standard solar abundance of the elements, other than H and He, that are considered by SYNSPEC v45). The new synthetic spectra were calculated using the modified composition procedure in SYNSPEC; the composition change list included all 28 metals treated by version 45 of SYNSPEC. Because the model atmospheres assumed a H-He composition, all lines except H and He are treated in LTE by SYNSPEC. For this stage of the fitting process, we rebinned the original *FUSE* spectrum to a dispersion of 0.1 Å pixel<sup>-1</sup> and utilized a 0.5 Å broadening function for the synthetic spectra. Refitting as described above, but using 2501 degrees of freedom, yielded a best value of  $Z \approx 0.5Z_{\odot}$ . Detailed examination of the spectral fits indicated that visual evaluation of individual spectral features gives a more sensitive determination of composition effects than the formal fit over the entire spectrum. This evaluation allowed us to refine the composition to  $Z \approx 0.3Z_{\odot}$  for the WD in MV Lyr.

In producing each fit we ignored wavelengths shortward of 930 Å. The *FUSE* spectrum shows

---

<sup>8</sup>Also see <http://tlusty.gsfc.nasa.gov/>.

a rapid drop in flux in that wavelength region that is in conflict with the synthetic spectra. A fit to the falling flux level shortward of 930 Å would require a  $T_{\text{eff}}$  at least 10,000 K cooler than the adopted value of 47,000 K, and the corresponding synthetic spectrum would be seriously discordant with the remainder of the *FUSE* spectrum at wavelengths longward of 930 Å. It is likely that the flux drop-off shortward of 930 Å is linked to an instrumental effect, since both LiF detectors have no sensitivity below about 1000 Å, the SiC2 detector has essentially zero effective area below  $\approx 920$  Å and the SiC1 detector does not reach peak effective area until  $\approx 940$  Å. We estimate that the fit to the *FUSE* spectrum has probable uncertainties of 1000 K in  $T_{\text{eff}}$  and 0.25 in  $\log g$ . It is of interest that the composition  $Z \approx 0.3Z_{\odot}$  found for MV Lyr differs markedly from the value of 0.71 derived for the novalike CV (and VY Scl star) DW Ursae Majoris (Araujo-Betancor et al. 2003).

### 3.1.1. Mass and Radius of the WD

We used the mass-radius relation for zero-temperature, carbon WD models (Hamada & Salpeter 1961) to locate a WD that corresponds to the  $\log g = 8.25$  indicated for MV Lyr. The carbon model with  $M_{\text{wd}} = 0.722M_{\odot}$  and  $R = 0.01067R_{\odot}$  has a photospheric  $\log g$  of 8.233, in close agreement with the MV Lyr  $\log g$  value. The difference between successive tabular values of WD mass in Hamada & Salpeter (1961) corresponds to an interval of about 0.25 in  $\log g$ , equal to the  $\log g$  spacing in our model atmosphere and synthetic spectrum grids. The mass difference between the selected model WD and adjacent models in Hamada & Salpeter (1961) is about  $0.1M_{\odot}$ , which we adopt as the uncertainty in the MV Lyr WD mass. Substitution of a helium WD produces only a very small difference in the mass and radius values.

### 3.1.2. Rotational Velocity and Detailed Composition of the WD

Determination of  $v_{\text{rot}} \sin i$  values for the WDs in CVs is important for understanding angular momentum transfer and braking phenomena. We did not attempt to determine a non-zero  $v_{\text{rot}} \sin i$  value for MV Lyr because our model spectrum analysis achieved an accurate fit to the *FUSE* spectrum while assuming a rotational velocity of zero and considering only  $T_{\text{eff}}$  and  $\log g$ . An independent analysis by one of us (E. M. S.), using NLTE model atmospheres calculated with TLUSTY (v200) and WD synthetic spectra calculated with SYNSPEC (v48), determined the following parameters:  $T_{\text{eff}} = 44,000$  K,  $\log g = 8.22$ ,  $v_{\text{rot}} \sin i = 200 \text{ km s}^{-1}$ , and detailed elemental abundances relative to solar values of C=0.5, N=0.5, and Si=0.2. The reduced  $\chi^2$  for this fit is 1.65 (compare to our full system fit discussed in Section 3.2 and Table 5). The EMS value of  $\log g$  is essentially identical to our result from Section 3.1, while the EMS value of  $T_{\text{eff}}$  is close to the 47,000 K value from Section 3.1 – the inclusion of  $v_{\text{rot}} \sin i$  in the EMS solution might explain the small  $T_{\text{eff}}$  difference. We note that both temperature values are in good agreement with the pre-TLUSTY  $T_{\text{eff}}$  of  $\sim 50,000$  K determined by Szkody & Downes (1982). The individual EMS chemical composition values are not inconsistent with the combined metallicity determined in Section 3.1. Our

independent analyses indicate that the WD in MV Lyr is a “slow rotator” (i.e., it is on the low side of the CV WD  $v_{\text{rot}} \sin i$  distribution). The chemical abundance ratio does not indicate that N is elevated above C; hence there is no evidence for CNO processing of the accreted material in the WD surface layers. Such processing is seen, for example, in the WDs in the dwarf novae U Geminorum (Long & Gilliland 1999) and VW Hydri (Sion et al. 1995, 2001).

### 3.2. Complete System Model

The initial synthetic spectrum analysis described in Section 3.1 provides us with parameters for the WD component in a complete system model that spans our FUV and optical spectroscopic data. We used the BINSYN software package (Linnell & Hubeny 1996) to produce this system model. BINSYN calculates separate synthetic spectra for the two stellar components, the accretion disk face, and the accretion disk rim (including an optional bright spot at the accretion stream impact site), as well as a composite system synthetic spectrum. It includes limb darkening on these components, as well as effects of orbital inclination and phase.

Calculation of the flux from the system depends sensitively on the representation of the WD. Production of the composite system spectrum, in the operating mode for the BINSYN module ACPGF6, requires a limb darkening value for each component that contributes to the composite spectrum. The source synthetic spectrum for the  $T_{\text{eff}} = 47,000$  K,  $\log g = 8.25$  model atmosphere provides intensities for a range of 10 values of  $\cos(\gamma)$  at each tabular wavelength. We used the tabulation at  $1050 \text{ \AA}$  to determine a linear limb darkening coefficient of 0.45. That value was used for the WD in calculating the composite system spectrum for comparison with the *FUSE* spectrum. For the secondary star component, we adopted  $T_{\text{eff}} = 3500$  K and  $\log g = 4.0$ , and used a Kurucz model atmosphere to calculate its synthetic spectrum. See Section 3.2.2 for a more detailed discussion of the secondary star.

An additional model parameter that must be specified is the mass transfer rate. Our WD-only synthetic spectrum fit to the *FUSE* spectrum has already ruled out a significant accretion disk contribution in the FUV. A fit to our optical wavelength spectra of MV Lyr (see Section 3.2.1) demonstrates that the contribution of an accretion disk is also negligible in the optical. Tests with a variety of assumed mass transfer rates led us to adopt a rate of  $3 \times 10^{-13} M_{\odot} \text{ yr}^{-1}$ . We show below (see Section 3.2.3) that this is a maximum acceptable mass transfer rate, and that the true rate in the present faint state of MV Lyr may actually be less than this.

The parameters of our final system model are listed in Table 4. The values of  $M_{\text{wd}}$ ,  $q$ ,  $i$ , and  $P_{\text{orb}}$  are from SPT95. The component separation is  $D$ , and subscripts “wd” and “s” refer to the WD and secondary star components, respectively. Bolometric albedos ( $A_{\text{wd}}$  and  $A_{\text{s}}$ ) are standard, as are the gravity brightening exponents ( $b_{\text{wd}}$  and  $b_{\text{s}}$ ). The Roche potentials ( $\Omega_{\text{wd}}$  and  $\Omega_{\text{s}}$ ) were fixed to correspond to the previously calculated size of the WD (see Section 3.1.1) and to cause the secondary star to fill its Roche lobe, respectively. Size parameters without listed units ( $r_{\text{wd}}$  and  $r_{\text{s}}$ )

are in units of the stellar component separation. The accretion disk outer radius ( $r_o$ ) was set equal to the tidal disruption radius. The disk rim semi-height ( $H$ ) is the standard model (Frank, King, & Raine 1992) value corresponding to the adopted mass transfer rate.

Figure 5 shows the *FUSE* spectrum of MV Lyr from Figure 4 with the synthetic spectrum calculated from our BINSYN system model superposed. The large-amplitude, narrow, positive features in the residuals panels are caused by the geocoronal emission lines in the *FUSE* spectrum, while the narrow negative features are caused by ISM absorption lines in the *FUSE* spectrum. Both types of feature are not reproduced in the model spectrum, and were masked off during the fitting process. Figure 5 is essentially indistinguishable from a corresponding plot (not shown) using only the SYNSPEC WD synthetic spectrum. Note that the C III  $\lambda 1176$  absorption complex shown in the bottom panel of the figure matches the model quite well, whereas the adjacent C IV  $\lambda 1169$  line is obscured by an airglow feature (which prevents its use as a temperature diagnostic).

Table 5 lists the fitting results (as described in Section 3.1) for the  $Z = 0.3Z_\odot$  composition,  $T_{\text{eff}} = 47,000$  K,  $\log g = 8.25$  WD model. The synthetic spectrum used is the BINSYN system synthetic spectrum. The fit used 2501 degrees of freedom. A corresponding calculation using just the SYNSPEC WD synthetic spectrum produced an identical quality fit, but differed in the scaling factor. The scaling factor for the system spectrum is needed to calculate the distance to MV Lyr (see Section 3.4).

### 3.2.1. Fit to the Optical Spectra

We used the intensity tabulation from the SYNSPEC WD-only spectrum at 4500 Å to determine a linear limb darkening coefficient of 0.15 for the WD over the wavelength range of our APO optical spectra. We then calculated an optical portion of the system model spectrum using BINSYN. Initial comparison between the BINSYN optical spectrum, which was scaled identically to the FUV portion that matches our *FUSE* data, and our APO optical spectra revealed that the flux levels of the latter are *below* the model flux. This is not unexpected, as the optical spectra were obtained through intermittent clouds and have an unreliable absolute flux calibration (see Section 2.2). Consequently, we scaled the optical spectra by a factor of 1.87 in order to match the blue optical spectrum (which is least affected by any contribution from the secondary star – see Section 3.2.2) to the BINSYN model spectrum. The corresponding BINSYN system spectrum is shown superposed on our scaled optical spectra in Figure 6. The maximum contribution of the secondary star component to the blue spectrum occurs at 5200 Å and amounts to 10% of the flux in the combined BINSYN spectrum. The calculated secondary star flux remains nearly constant over the interval 6000–7800 Å, while the contribution of the WD gradually decreases. At 7800 Å, the secondary star contributes 60% of the combined system flux. The contribution of a possible accretion disk in the BINSYN spectrum is negligible in the APO blue spectrum and very small in the red spectrum.

### 3.2.2. The Secondary Star

SYS81 determined a spectral type of M5 for the secondary star in MV Lyr, based on infrared spectra. This classification implies  $T_{\text{eff}} = 2800$  K for the secondary star (Reid & Hawley 2000). SPT95 determined a secondary star mass of  $0.3M_{\odot}$  (and a mass ratio  $q = 0.43$ ) from dynamic considerations. This mass corresponds to  $T_{\text{eff}} = 3200$  K (Reid & Hawley 2000). However, the current distribution version of TLUSTY (v200) can not calculate photospheric models for stars cooler than 5500 K (because of the lack of molecular opacities), and the coolest model in the Kurucz grid has  $T_{\text{eff}} = 3500$  K. Consequently, we adopted  $T_{\text{eff}} = 3500$  K and  $\log g = 4.0$  for the secondary star. BINSYN includes an evaluation of irradiative heating of the secondary star by the WD and accretion disk, including effects of shadowing in the equatorial region of the secondary star by the accretion disk. However, inclusion of those calculated effects in an initial iteration of our MV Lyr model produced too large a contribution from the secondary star. The slope of the resulting system synthetic spectrum was too small compared to the blue APO spectrum, for any normalizing factor. Similarly, the synthetic spectrum had too much flux at long wavelengths to fit the red APO spectrum, using a single normalizing factor for both the blue and red spectra. We conclude that the  $T_{\text{eff}}$  of the secondary must be cooler than the 3500 K adopted in our model. This conclusion is consistent with the inferred secondary star temperatures from SYS81 and SPT95. As mentioned by SYS81, the secondary star in MV Lyr may be even cooler than a normal main sequence star of its mass. If this is the case, then the SYS81 temperature might still be appropriate for the SPT95 mass. The lower temperature in either case will result in an even smaller contribution to the FUV and optical spectra than we have assumed.

Because we have used a single 3500 K source spectrum for the secondary star, that component's photospheric representation is forced to be isothermal. We believe that a 2800 K model atmosphere would provide a source synthetic spectrum, when corrected for irradiation, that the present isothermal source spectrum approximates. No substantial contribution to the blue optical spectrum can be allowed from either the secondary component or an accretion disk. Such a contribution reduces the slope of the synthetic spectrum and quickly produces discordance with the observed spectrum. This discordance is distinct from the vertical translation produced by the normalizing factor used to superpose the observed and synthetic spectra. The very slight extra flux in the APO spectrum longward of 7300 Å (excluding the atmospheric absorption feature at  $\lambda \approx 7600$  Å – see Figure 6) may be an unrepresented signature of the secondary component. Roughly half of the photons emitted by the WD have wavelengths shortward of the Lyman limit. This same fraction of the irradiative photons absorbed by the secondary star will ionize H atoms. Consequently, the Balmer emission lines in MV Lyr are probably recombination lines from the secondary component (as concluded also by Robinson et al. 1981 and SPT95).

### 3.2.3. Constraints on the Accretion Disk

BINSYN calculates a standard model accretion disk (Frank, King, & Raine 1992) corresponding to a given mass transfer rate. The BINSYN program includes an option to approximate irradiative heating of the accretion disk faces by the WD. The calculation uses the bolometric albedo formalism conventionally applied to evaluate component irradiation in classical binary systems. A much better approximation is available, using source synthetic spectra of individual annuli, calculated with TLUSTY (v200) (Hubeny 1989, 1990, 1991), but this level of sophistication is unnecessary in view of the extremely small contribution of an accretion disk, if one even exists in MV Lyr in the faint state. In general, we found that the contribution of an accretion disk, if present, is negligible in MV Lyr. We verified this conclusion as described below.

If we included irradiation of the disk in our BINSYN model calculation, on the very crude bolometric albedo formalism, then the calculated flux from the accretion disk faces arising from irradiation by the WD would dominate the emission from the faces. The inner annuli would reach  $T_{\text{eff}}$  values that are roughly a factor of four higher than the standard model  $T_{\text{eff}}$  values for an accretion rate of  $3 \times 10^{-13} M_{\odot} \text{yr}^{-1}$  (16,000 K vs. 4000 K). Because of the temperature dominance by the WD, the emitted flux from the accretion disk is insensitive to the adopted rate of mass transfer. If we include irradiation effects, then the calculated flux from the accretion disk in our model would be twice the flux from the WD in the spectral interval 3900–5200 Å, a condition excluded by the observed blue optical spectrum. A possible solution for this discrepancy (other than concluding that there is no significant accretion disk in MV Lyr) is that the inner accretion disk is dissipated by the radiation field of the WD or is truncated by a magnetic field associated with the WD. However, even truncating the accretion disk at 3 times the WD radius does not solve the problem. On the other hand, if irradiation by the WD is ignored, the standard model flux from an accretion disk with the mass transfer rate specified above is 1/8 the flux from the secondary star at 7800 Å, and so makes a negligible contribution to the spectra, as required by the observations. Even though our irradiation calculation is crude, we believe it is safe to conclude that the mass transfer rate during the current faint state of MV Lyr is no larger than the  $3 \times 10^{-13} M_{\odot} \text{yr}^{-1}$  adopted in our model, and is possibly even smaller. Hubeny (1990) has considered irradiation of accretion disks on a more sophisticated basis, and Hubeny (1991) presents examples of the effects of irradiation. Our simplified approach is justified by the absence of a detectable accretion disk in MV Lyr.

We used our BINSYN model to calculate a synthetic optical light curve for MV Lyr under the assumption that no accretion disk is present in the system. That light curve is shown with the second night of our optical photometry (bottom panel of Figure 2) in Figure 7. The amplitude of the sinusoidal modulation in the model light curve is approximately 50% too large compared to the observed optical data. The amplitude is strongly dependent on irradiation of the secondary star near the L1 point. Shielding by a nascent accretion disk could reduce the amplitude. Alternatively, since the mass transfer rate is very small, the secondary star could be slightly detached from its Roche lobe, with a smaller irradiative effect near the L1 point.

### 3.3. Ultraviolet Spectra of MV Lyr

MV Lyr was observed with *IUE* several times between 1979–1988, in both the faint and bright accretion states. All spectra were obtained at low resolution using the *IUE* large aperture. The short wavelength (SWP) spectra span a usable wavelength range of 1185–1980 Å with a dispersion of 1.7 Å pixel<sup>-1</sup>, while the long wavelength (LWR) spectra span a usable range of 1980–3000 Å with dispersion of 2.7 Å pixel<sup>-1</sup>. We retrieved several of these spectra from the *IUE* archive for comparison with our observed and model spectra (see Table 6). The faint state *IUE* spectra were chosen such that the short wavelength end of the SWP spectrum matches the flux level of the long wavelength end of our *FUSE* spectrum, while the bright state spectra are simply the archived *IUE* spectra with the largest flux. In both cases, the LWR spectra are those obtained on the same day as the corresponding SWP spectra, to ensure that they represent the same accretion state of MV Lyr. The bright and faint state spectra were originally presented by Szkody & Downes (1982) and Chiappetti et al. (1982), respectively. Figure 8 shows our *FUSE* and optical spectra coplotted with the *IUE* spectra, both alone (top panel) and with the BINSYN model spectrum overplotted (bottom panel). The faint state *IUE* spectra match the 1200–3000 Å region of the model spectrum very well, providing additional, independent confirmation of our model. By comparison, the bright state *IUE* spectra have a much higher flux level and significantly flatter continuum slope.

### 3.4. Distance to MV Lyr

The scaling factor between the observed FUV spectrum and BINSYN model spectrum is  $S_B = 2.43 \times 10^{42}$ . The flux output of BINSYN is  $H_{\text{binsyn}} = (4\pi r^2)H_\lambda$ , where  $H_\lambda$  is the Eddington flux. Thus, the observed flux,  $f_\lambda$ , is related to the BINSYN model flux as

$$f_\lambda = (4\pi)(r^2/d^2)H_\lambda = H_{\text{binsyn}}/d^2. \quad (1)$$

The distance,  $d$ , to MV Lyr can then be estimated from the scaling factor as  $d = \sqrt{S_B}$ , which gives  $d = 505$  pc (assuming no interstellar absorption). The estimated uncertainty in this distance is 50 pc<sup>9</sup>.

We repeated the distance estimate by calculating the scaling factor ( $S_S = 3.20 \times 10^{23}$ ) required to fit the SYNSPEC WD-only spectrum (which is in units of the Eddington flux,  $H_\lambda$ ) to the observed *FUSE* spectrum, under the demonstrated assumption that there is no significant contribution to the

---

<sup>9</sup>Strictly speaking, the equations for  $H_\lambda$  and  $f_\lambda$  used here are only true in the case of a single spherical star. This is a good assumption for the FUV observations of MV Lyr, which contain only a contribution from the naked WD. In general, however, BINSYN can handle more complex cases in which the star is tidally or rotationally distorted, and/or the observed flux contains contributions from two stars plus an accretion disk. Even in such a complicated system, comparison of the observed and calculated fluxes still correctly yields the distance to the system.

FUV spectrum of MV Lyr from sources other than the WD. We utilized the WD radius determined by the BINSYN model (see Table 4). This calculation results in  $d = 512$  pc, consistent with the distance estimate obtained from the BINSYN scaling factor.

SYS81 determined a distance to MV Lyr of 322 pc from infrared observations. They note that if the secondary star is cooler than expected for its mass, assuming it is a main sequence star, then their distance determination is an underestimate. If the SYS81 temperature of  $T_{\text{eff}} = 2800$  K is correct, then the ratio of our distance estimate to theirs implies that the radius of the secondary star can be up to a factor of  $\approx 1.6$  larger than that of an M5 star without exceeding its current flux contribution to the total system spectrum. This assumes that size is the only factor that would contribute to a difference in the flux contributed by the secondary star. If the secondary star temperature is higher, as proposed by SPT95, then the allowable increase in size relative to the “normal” radius for the spectral class corresponding to that temperature will be smaller.

#### 4. Conclusions

We have presented the first FUV spectrum of MV Lyr, along with contemporaneous optical light curves and spectra. All of the data were obtained during a deep, faint accretion state of this novalike CV. The optical light curve displays a sinusoidal modulation on the orbital period of MV Lyr. Power spectrum analysis reveals no other coherent signal in the light curve. The optical spectra display prominent, narrow emission lines of H I and He I that likely originate on the irradiated secondary star. Broad absorption troughs originating from the WD are present in the  $H\beta$  and higher series Balmer lines. The He II  $\lambda 4686$  line is present purely in absorption. The FUV spectrum contains a mix of broad (H I and He II) and narrow (C, N, Si, S) absorption features (as well as some contamination from geocoronal emission and interstellar absorption).

We used a grid of synthetic spectra, fitted individually to our *FUSE* spectrum, to determine  $T_{\text{eff}} = 47,000$  K,  $\log g = 8.25$ , and  $Z = 0.3Z_{\odot}$  for the WD in MV Lyr. We then used the BINSYN software package to compute a faint state system model for MV Lyr based on our FUV and optical spectra. This model includes the 47,000 K WD, a 3500 K secondary star, and essentially no contribution from a standard model accretion disk. Detailed modelling of the WD chemical abundances shows no evidence for CNO processing of accreted material. The upper limit of the mass transfer rate in this CV is  $3 \times 10^{-13} M_{\odot} \text{ yr}^{-1}$ , based on its resulting flux contribution if irradiation of the accretion disk by the WD is neglected. Although not used in the formal BINSYN fitting process, archival faint state *IUE* spectra of MV Lyr are well-matched by the BINSYN model spectrum in the 2000–3000 Å region.

The BINSYN model spectrum demonstrates that the WD contributes all of the flux in the FUV, and from 90% at 5200 Å to 40% at 7800 Å in the optical. The secondary star temperature of 3500 K was adopted out of necessity, as this is the coolest available model atmosphere; however, the inability to include irradiative heating effects in the model without producing disagreement

with the observed optical spectra implies that the true temperature of the secondary star is lower. The scaling factor between the BINSYN model spectrum and the observed *FUSE* spectrum allows us to calculate a distance of  $d = 505 \pm 50$  pc. A previous distance estimate of 322 pc (SYS81) is likely a lower limit if the secondary star in MV Lyr is too cool for its mass.

A model optical light curve computed from the BINSYN model for MV Lyr, under the assumption that no accretion disk is present, has an amplitude that is approximately 50% larger than that of the sinusoidal modulation in the observed optical light curve. Shielding by a nascent disk and/or less irradiation of the secondary star near the L1 point (due to it being slightly detached from its Roche lobe) could reduce the amplitude of the modulation in the light curve.

This research was supported by NASA *FUSE* grant NAG5-12203, including travel by I. H. to the University of Washington to facilitate his participation. Participation by E. M. S., as well as computational assistance from F.-H. Cheng, was supported by NASA grant 5-12067. The research described in this paper was carried out, in part, at the Jet Propulsion Laboratory, California Institute of Technology, and was sponsored by the National Aeronautics and Space Administration. In this research, we have used, and acknowledge with thanks, data from the AAVSO International Database, based on observations submitted to the AAVSO by variable star observers worldwide. Some of the data presented in this paper were obtained from the Multimission Archive at the Space Telescope Science Institute (MAST). STScI is operated by the Association of Universities for Research in Astronomy, Inc., under NASA contract NAS5-26555. Support for MAST for non-HST data is provided by the NASA Office of Space Science via grant NAG5-7584 and by other grants and contracts. We made use of the SIMBAD database, operated at CDS, Strasbourg, France.

## REFERENCES

- Araujo-Betancor, S. et al. 2003, *ApJ*, 583, 437
- Chiappetti, L., Maraschi, L., Tanzi, E. G., & Treves, A. 1982, *ApJ*, 258, 236
- Feldman, P. D., Sahnou, D. J., Kruk, J. W., Murphy, E. M., & Moos, H. W. 2001, *J. Geophys. Res.*, 106, 8119
- Frank, J., King, A., & Raine, D. 1992, *Accretion Power in Astrophysics* (Cambridge: Univ.Press)
- Hamada, T. & Salpeter, E. E. 1961, *ApJ*, 134, 683
- Henden, A. A. & Honeycutt, R. K. 1995, *PASP*, 107, 324
- Hubeny, I. 1988, *Comp. Phys. Comm.*, 52, 103
- Hubeny, I. 1989, in *Theory of Accretion Disks*, eds. F. Meyer, et al. (Dordrecht: Kluwer)
- Hubeny, I. 1990, *ApJ*, 351, 632

- Hubeny, I. 1991, in *Structure and Emission Properties of Accretion Disks*, eds. C. Bertout et al. (Singapore: Fong & Sons), 227
- Hubeny, I. & Lanz, T. 1995, *ApJ*, 439, 875
- Hubeny, I., Stefl, S., & Harmanec, P. 1985, *Bull. Astron. Inst. Czechosl.* 36, 214
- Linnell, A. P. & Hubeny, I. 1996, *ApJ*, 471, 958
- Long, K. S. & Gilliland, R. L. 1999, *ApJ*, 511, 916
- Reid, L. N. & Hawley, S. L. 2000, *New Light on Dark Stars* (Berlin: Springer), 149
- Roberts, D. H., Lehár, J., & Dreher, J. W. 1987, *AJ*, 93, 968
- Robinson, E. L., Barker, E. S., Cochran, A. L., Cochran, W. D., & Nather, R. E. 1981, */apj*, 251, 611
- Sahnou, D. J. et al. 2000, *Proc. SPIE*, 4013, 334
- Schneider, D. P., Young, P., & Shectman, S. A. 1981, *ApJ*, 245, 644 (SYS81)
- Sion, E. M., Cheng, F., Szkody, P., Gänsicke, B., Sparks, W. M., & Hubeny, I. 2001, *ApJ*, 561, L127
- Sion, E. M., Szkody, P., Cheng, F., & Huang, M. 1995, *ApJ*, 444, L97
- Skillman, D. R., Patterson, J., & Thorstensen, J. R. 1995, *PASP*, 107, 545 (SPT95)
- Szkody, P., & Downes, R. A. 1982, *PASP*, 94, 328
- Warner, B. 1995, *Cataclysmic Variable Stars* (Cambridge: Cambridge University Press)

Table 1. *FUSE* Observation Log

Exposure #	Start Time (HJD-2450000)	Total Exposure (s)	$\phi^a$
1	2463.000006	1664	0.470
2	2463.052124	3159	0.862
3	2463.120621	3240	1.378
4	2463.189985	3146	1.900

<sup>a</sup>Orbital phase at start of exposure from the spectroscopic ephemeris of SPT95.

Table 2. Lines in the FUV Spectrum of MV Lyr

Line	$\lambda_{\text{obs}}$ (Å)	Gaussian Fit:			Notes
		EW (Å)	EW (Å)	FWHM (km s <sup>-1</sup> )	
H I $\lambda$ 937.80	938.0	1.71	1.64	3.02	1, 2
H I $\lambda$ 949.74	950.7	4.27	4.51	6.91	1, 2
H I $\lambda$ 972.54	972.5	6.37	6.48	9.97	1, 2
He II $\lambda$ 992.36	992.1	1.89	1.97	7.30	1
N III $\lambda$ 1006.01	1006.2	0.12	0.13	0.68	3
H I $\lambda$ 1025.77	1025.8	10.21	9.59	13.2	1, 2
Si IV $\lambda$ 1066.62	1066.6	0.68	0.53	1.13	4
S IV $\lambda$ 1072.97	1073.1	0.22	0.23	1.09	5
He II $\lambda$ 1084.94	1085.0	4.52	4.17	7.86	6
C IV $\lambda$ 1107.83	1107.7	0.33	0.33	1.18	5, 7
P V $\lambda$ 1117.98	1117.9	0.21	0.23	1.29	8
Si IV $\lambda$ 1122.48	1122.4	0.36	0.36	0.83	...
P V $\lambda$ 1128.01	1127.9	0.07	0.02	0.80	9
Si IV $\lambda$ 1128.33	1128.5	0.24	0.31	0.94	9
Si III $\lambda$ 1144.31	1144.9	0.34	...	...	10
C III $\lambda$ 1175.6	1175.5	1.20	1.26	1.93	5

Note. — (1) Strong interstellar absorption and/or airglow masked off. (2) Possibly blended with an He II absorption line. (3) Possibly blended with Si III  $\lambda$ 1005.37. (4) Blended with interstellar Ar I  $\lambda$ 1066.66. (5) Blend of multiplet transitions of this ion. (6) Affected by unmasked interstellar absorption and/or airglow. (7) Possibly blended with Si III  $\lambda$ 1108.36. (8) Possibly blended with S IV  $\lambda$ 1117.16. (9) Gaussian fit is deblend using “d” routine in IRAF task “splot.” (10) Blended with interstellar Fe II  $\lambda$ 1144.94.

Table 3. ISM Lines in the FUV Spectrum of MV Lyr

Line	$\lambda_{\text{obs}}$ ( $\text{\AA}$ )	EW ( $\text{\AA}$ )	Notes
H I $\lambda$ 919.35	919.4	0.41	...
H I $\lambda$ 920.96	920.9	0.32	...
H I $\lambda$ 923.15	923.1	0.29	...
H I $\lambda$ 926.23	926.2	0.21	...
O I $\lambda$ 948.69	948.5	0.30	...
O I $\lambda$ 950.88	950.9	0.16	...
N I $\lambda$ 952.4	952.5	0.15	1
N I $\lambda$ 953.6	953.6	0.19	1
N I $\lambda$ 954.0	954.0	0.14	1
N I $\lambda$ 963.99	963.9	0.22	2
N I $\lambda$ 964.63	964.6	0.11	...
N I $\lambda$ 965.04	965.0	0.12	...
O I $\lambda$ 976.45	976.4	0.18	3
C II $\lambda$ 1009.86	1009.7	0.07	...
C II $\lambda$ 1010.2	1010.1	0.09	1
Si II $\lambda$ 1020.70	1020.6	0.13	...
C II $\lambda$ 1036.34	1036.2	0.36	...
C II $\lambda$ 1037.02	1037.0	0.09	...
O I $\lambda$ 1039.23	1039.1	0.10	...
Ar II $\lambda$ 1048.22	1048.2	0.11	...
Fe II $\lambda$ 1063.18	1063.1	0.11	4

Note. — (1) Blend of multiplet transitions of this ion. (2) Possibly blended with interstellar P II  $\lambda$ 963.80. (3) Possibly blended with C III  $\lambda$ 977.02. (4) Blended with (unmeasurable) S IV  $\lambda$ 1062.66.

Table 4. BINSYN Model System Parameters

Parameter	Value	Parameter	Value
$M_{\text{wd}} (M_{\odot})$	0.73	$r_{\text{wd}}$	0.01017
$q (= M_2/M_{\text{wd}})$	0.43	$\log g_{\text{wd}}$	8.25
$P_{\text{orb}} (\text{d})$	0.1329	$r_{\text{s}} (\text{pole})$	0.28782
$D (R_{\odot})$	1.11323	$r_{\text{s}} (\text{point})$	0.40364
$\Omega_{\text{wd}}$	98.74	$r_{\text{s}} (\text{side})$	0.30011
$\Omega_{\text{s}}$	2.74	$r_{\text{s}} (\text{back})$	0.33258
$i (^{\circ})$	12	$\log g_{\text{s}} (\text{pole})$	4.95
$T_{\text{eff,p}} (\text{K})$	47,000	$\log g_{\text{s}} (\text{point})$	3.61
$T_{\text{eff,s}} (\text{K})$	3500	$\log g_{\text{s}} (\text{side})$	4.87
$A_{\text{wd}}$	1.0	$\log g_{\text{s}} (\text{back})$	4.68
$A_{\text{s}}$	0.5	$r_{\text{a}} (R_{\odot})$	0.52
$b_{\text{wd}}$	0.25	$r_{\text{b}} (R_{\odot})$	0.02
$b_{\text{s}}$	0.08	$H (R_{\odot})$	0.0027
		$\dot{M} (M_{\odot} \text{ yr}^{-1})$	$3 \times 10^{-13}$

Table 5. BINSYN Model Fit Results

Scale Factor ( $S \times 10^{-42}$ )	$\bar{r}_i$	$ \bar{r}_i $	$\sigma_r$	$\chi^2$	$\tilde{\chi}^2$
2.14	-0.4697	0.6373	0.6448	3828	1.5309
2.18	-0.4060	0.5983	0.6405	3505	1.4020
2.21	-0.3444	0.5644	0.6368	3232	1.2926
2.25	-0.2847	0.5362	0.6336	3005	1.2021
2.29	-0.2269	0.5137	0.6308	2824	1.1295
2.32	-0.1709	0.4958	0.6284	2685	1.0740
2.36	-0.1166	0.4827	0.6263	2587	1.0347
2.39	-0.0639	0.4743	0.6247	2526	1.0105
2.43	-0.0127	0.4711	0.6234	2501	1.0004
2.46	0.0369	0.4718	0.6223	2509	1.0035
2.50	0.0852	0.4769	0.6216	2547	1.0188
2.54	0.1321	0.4852	0.6211	2613	1.0452
2.57	0.1777	0.4971	0.6208	2705	1.0819
2.61	0.2220	0.5118	0.6208	2820	1.1279
2.64	0.2652	0.5285	0.6210	2956	1.1824
2.68	0.3071	0.5461	0.6214	3111	1.2444
2.71	0.3480	0.5650	0.6219	3283	1.3133
2.75	0.3879	0.5850	0.6226	3471	1.3883

Table 6. IUE Spectra of MV Lyr

Data ID	Start Time	Exposure Time (sec)	Accretion State
SWP 10905	1980 Dec 27 11:29:00	2400	faint
LWR 09590	1980 Dec 27 15:50:00	7080	faint
SWP 07296	1979 Dec 02 12:09:00	5400	bright
LWR 06288	1979 Dec 02 18:52:00	4200	bright

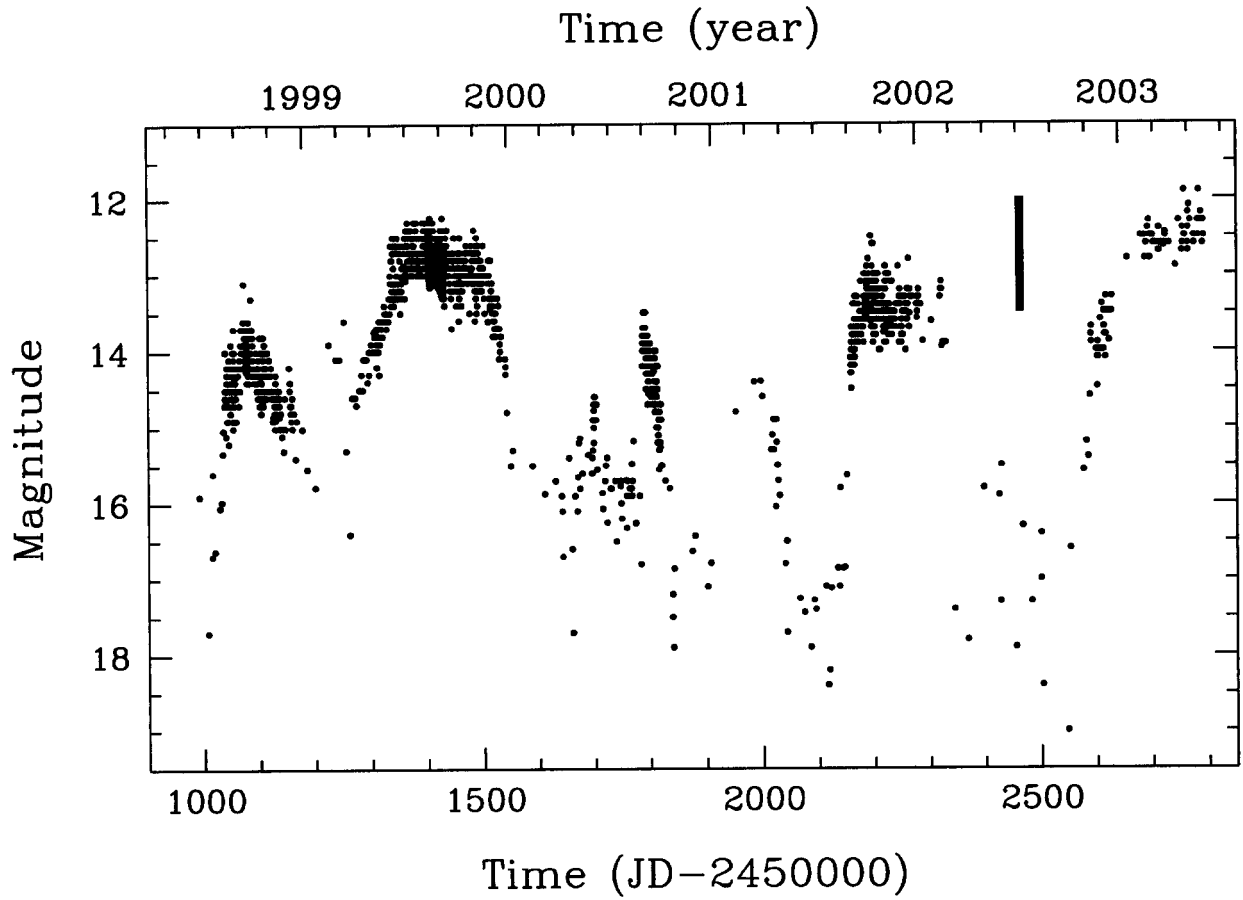


Fig. 1.— Long-term AAVSO light curve of MV Lyr. Only validated data are plotted (uncertain points and lower limits have been excluded). The vertical bar at year  $\approx 2002.5$  shows the date of our optical and far-UV observations of MV Lyr.

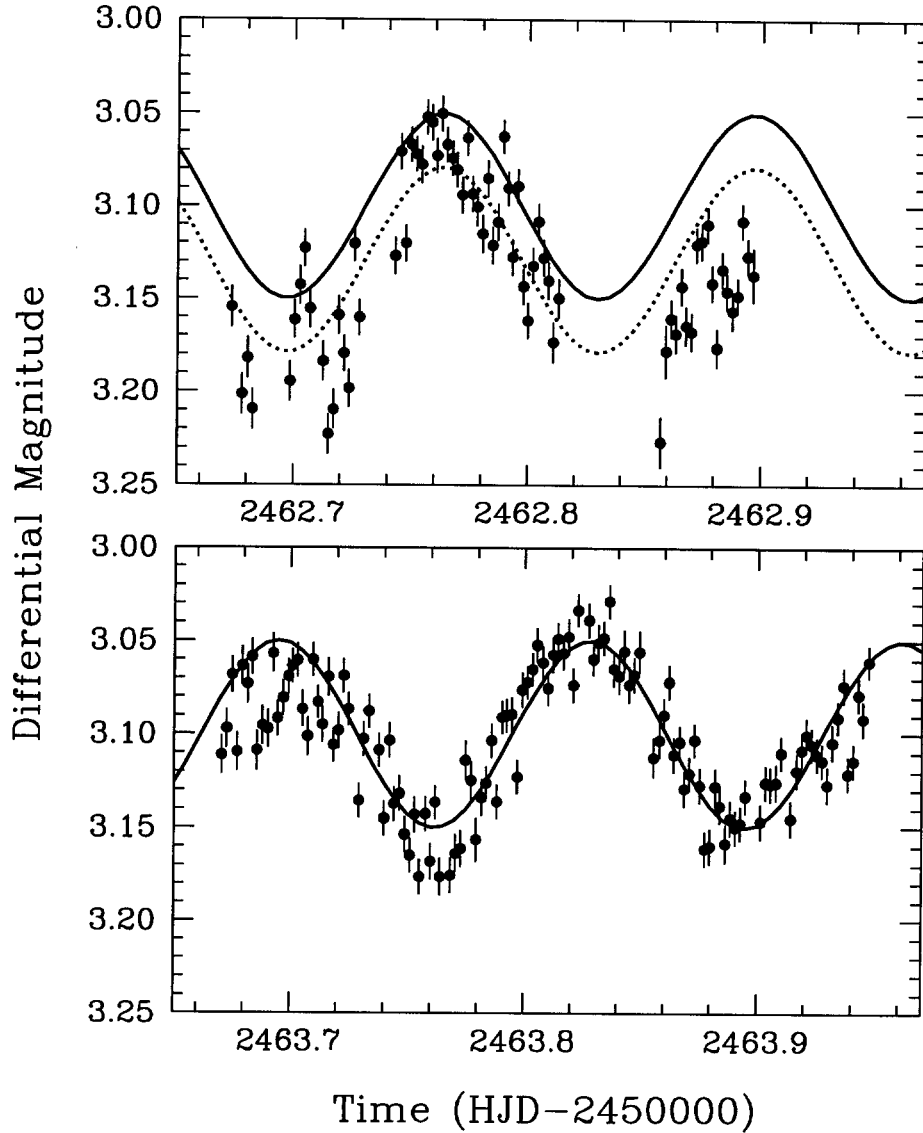


Fig. 2.— Differential light curves of MV Lyr in a faint state, from 2002 July 07 UT (top panel) and 2002 July 08 UT (bottom panel). The  $1\sigma$  uncertainties of the photometric data are shown. The solid curve shows the best sine function fit to the July 08 data, with a period of 0.1330 d (which is equivalent to the orbital period of MV Lyr within the 0.0019 d uncertainty of the sine fit). The dotted curve in the top panel is the same fit shifted by the 0.03 mag difference between the mean magnitude from each night.

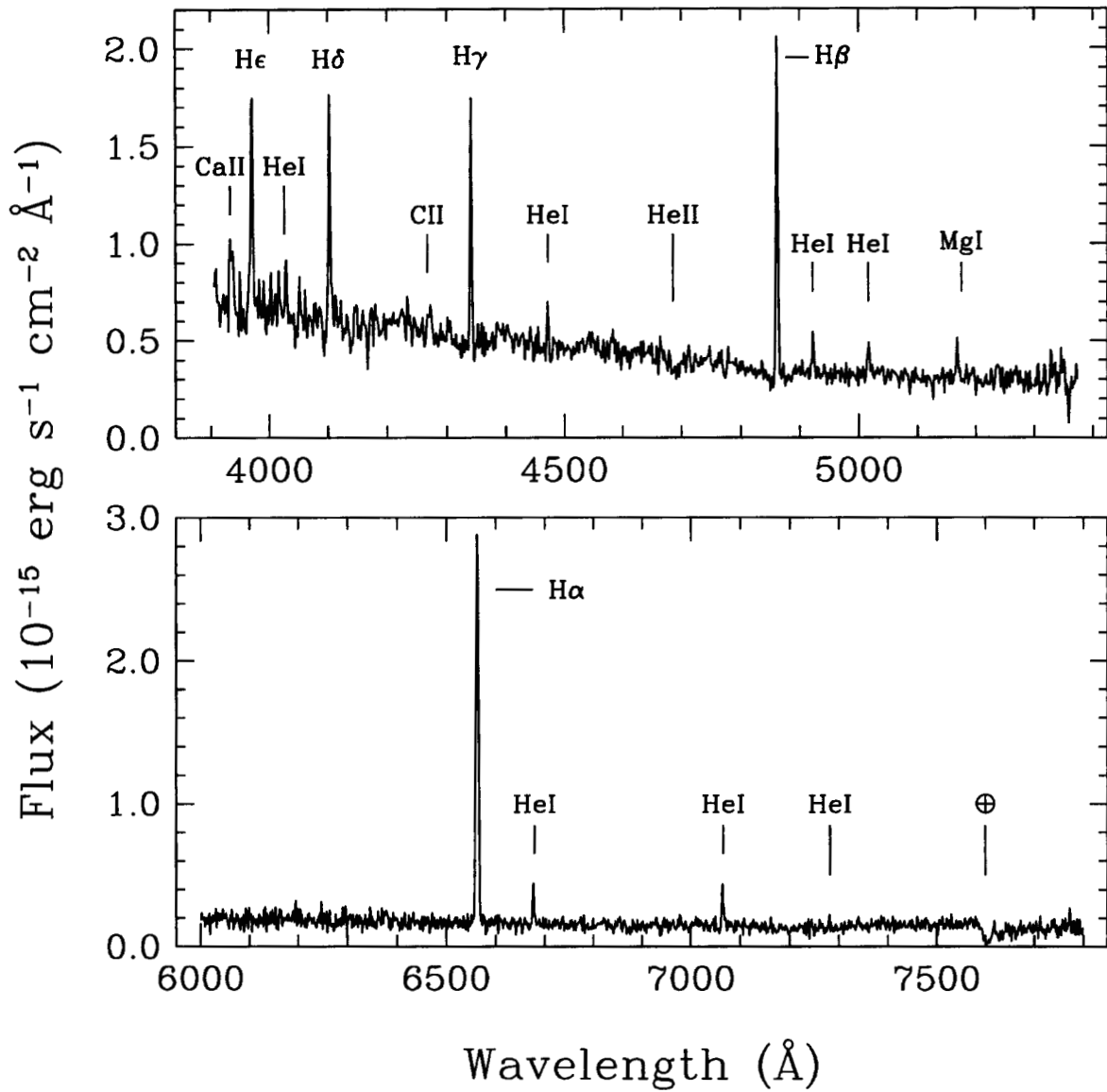


Fig. 3.— APO blue (top) and red (bottom) optical spectra of MV Lyr during the faint state, from 2002 July 03 UT. Ionic species of prominent emission lines are labeled. The spectrum flux has been multiplied by 1.87 to account for the presence of intermittent clouds (see Section 3.2.1 for derivation of this scaling factor).

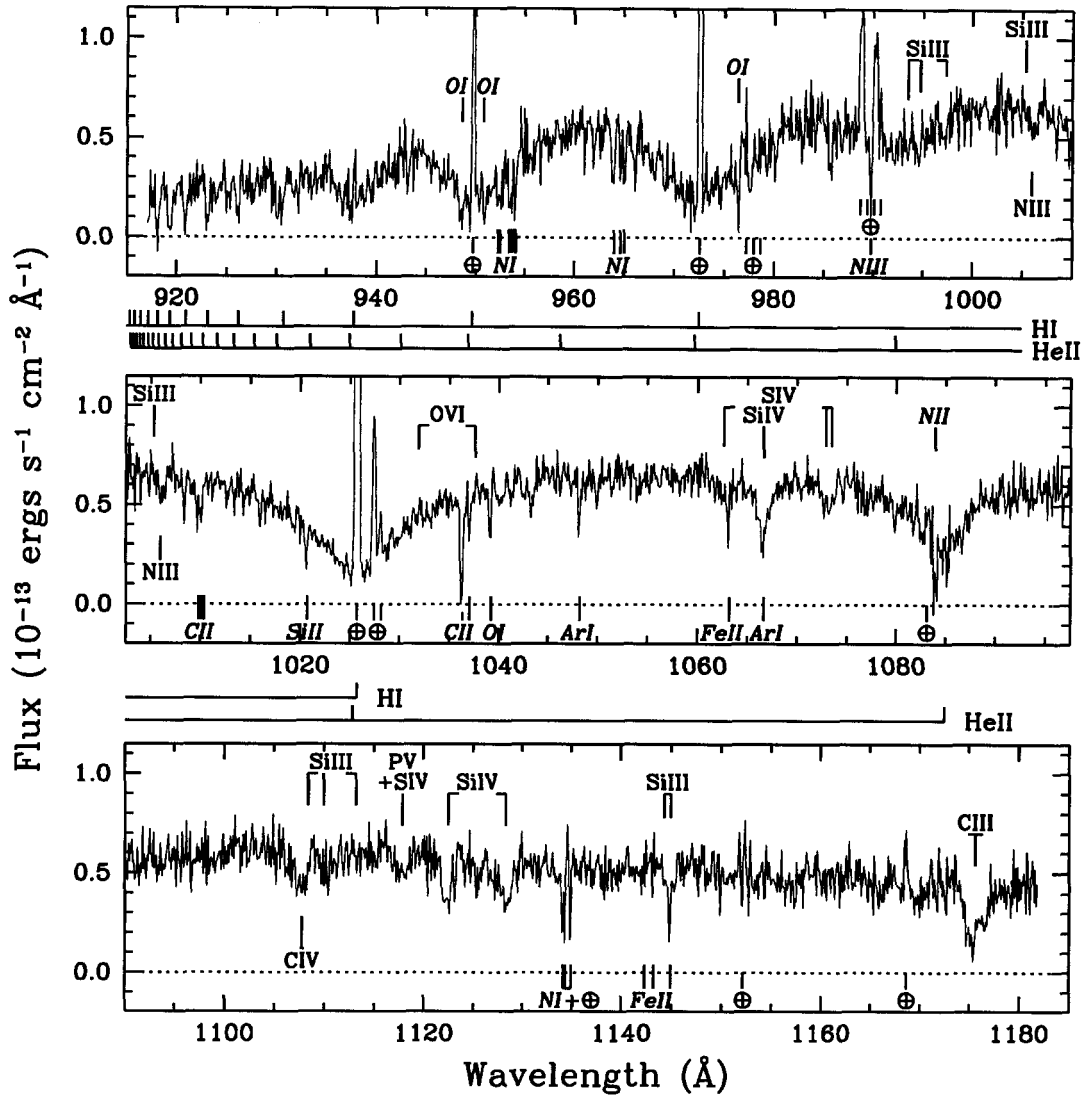


Fig. 4.— Total combined FUV spectrum of MV Lyr, binned to a dispersion of  $0.1 \text{ \AA pixel}^{-1}$ . The spectrum spans  $915\text{--}1185 \text{ \AA}$ ; the top and bottom panels overlap the ends of the middle panel by  $7.5 \text{ \AA}$ . Emission lines are labeled, with widely spaced lines of the same multiplet indicated by short horizontal bars on the “bookend” transitions, and multiplets with many closely spaced lines indicated by a vertical pointer at the midpoint wavelength joined to a horizontal bar spanning the multiplet transition wavelengths. Not all indicated lines are present in the spectrum; for example, the O VI lines at  $1032$  and  $1038 \text{ \AA}$  – which are common in FUV spectra of CVs – are conspicuously absent in our *FUSE* spectrum of MV Lyr. Airglow lines ( $\oplus$ ; identified from Feldman et al. 2001) and ISM lines (ions in italics) are indicated below the spectrum. The airglow lines have been truncated at the upper flux limit of the plot. Wavelengths of H I and He II transitions are shown outside and below the top and middle panels.

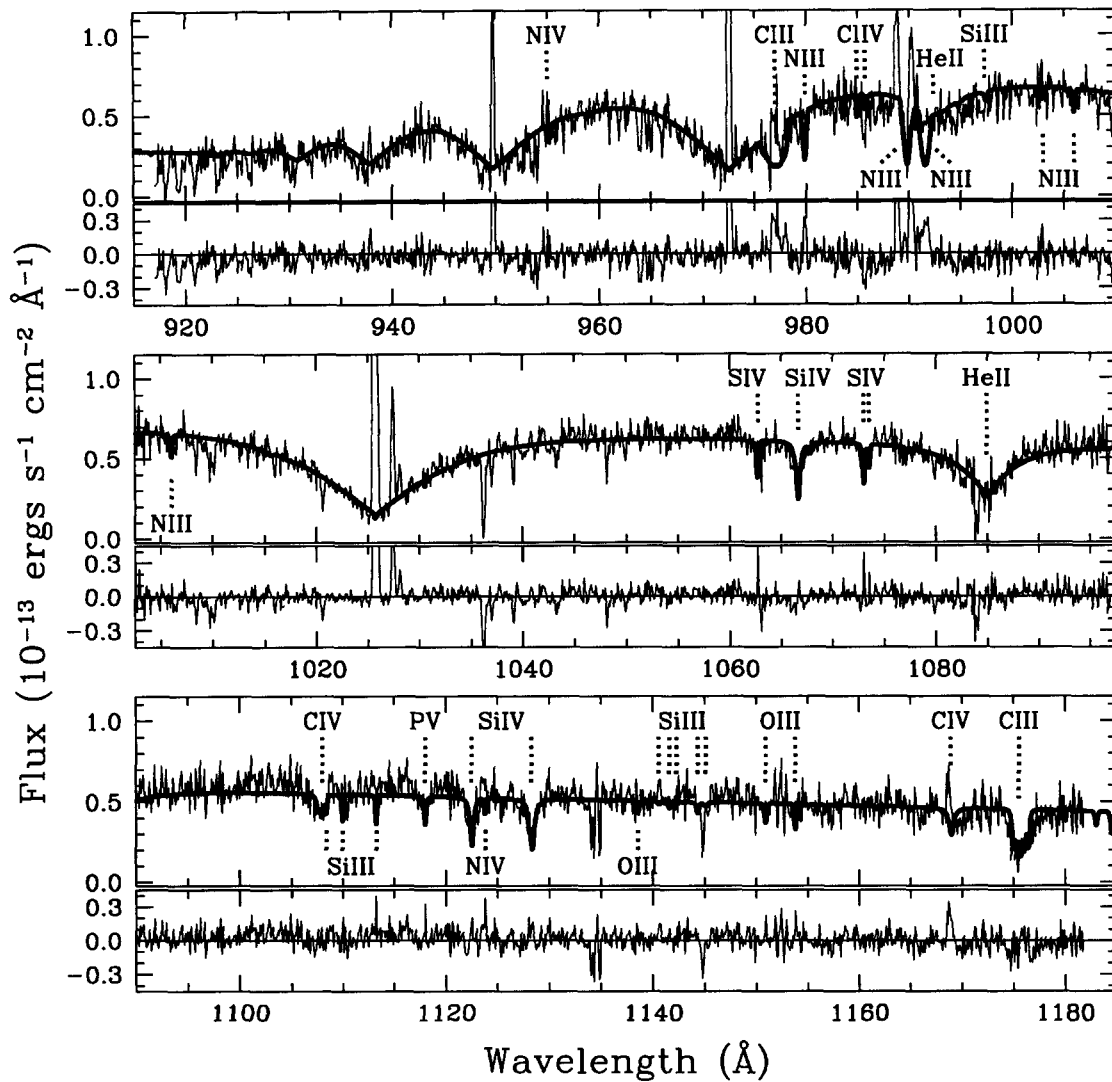


Fig. 5.— As in Figure 4, but with the best-fitting system model spectrum overplotted as a thick (blue) line. The model spectrum has an initial dispersion of  $0.01 \text{ \AA pixel}^{-1}$ , but was convolved with a Gaussian broadening function of  $\text{FWHM} = 0.2 \text{ \AA}$  to match the resolution of the plotted *FUSE* spectrum. The small panels below each spectrum panel show the ( $O - C$ ) difference between the observed spectrum ( $O$ ) and the calculated model spectrum ( $C$ ). Prominent atomic features in the *model* spectrum (except for the deep, broad H I absorption lines) are indicated; some of these features are not easily visible in the observed spectrum (in particular, the observed C II  $\lambda 977$  and C IV  $\lambda 1169$  lines are at least partially obscured by nearby airglow features). Data from wavelengths shortward of  $930 \text{ \AA}$  were not used in the model fits. The large-amplitude, positive features (caused by geocoronal emission lines in the observed spectrum) have been truncated at the upper flux limit of the plot panels.

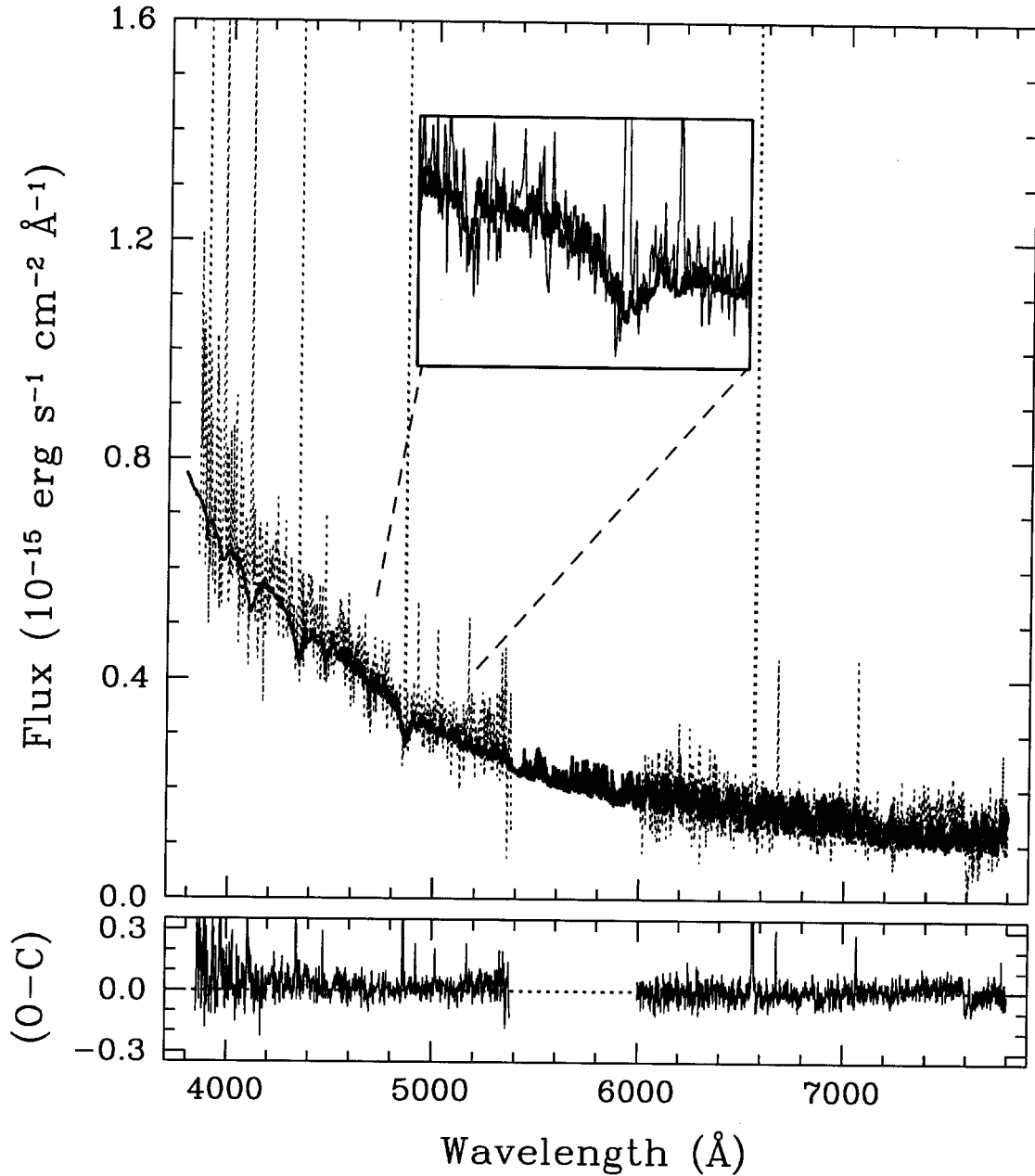


Fig. 6.— Main panel shows the optical spectra from Figure 3 (dotted line in print version; solid line in electronic version) with the BINSYN model spectrum (solid black line in print version; blue line in electronic version) superposed. The inset panel is an expanded view of the region around the He II  $\lambda 4686$  and H $\beta$  lines, showing the corresponding WD photospheric absorption features. The bottom panel is the  $(O - C)$  residual between the observed optical spectra ( $O$ ) and the calculated model spectrum ( $C$ ). The “discontinuity” at  $\lambda \approx 7600$  Å is caused by an atmospheric absorption feature.

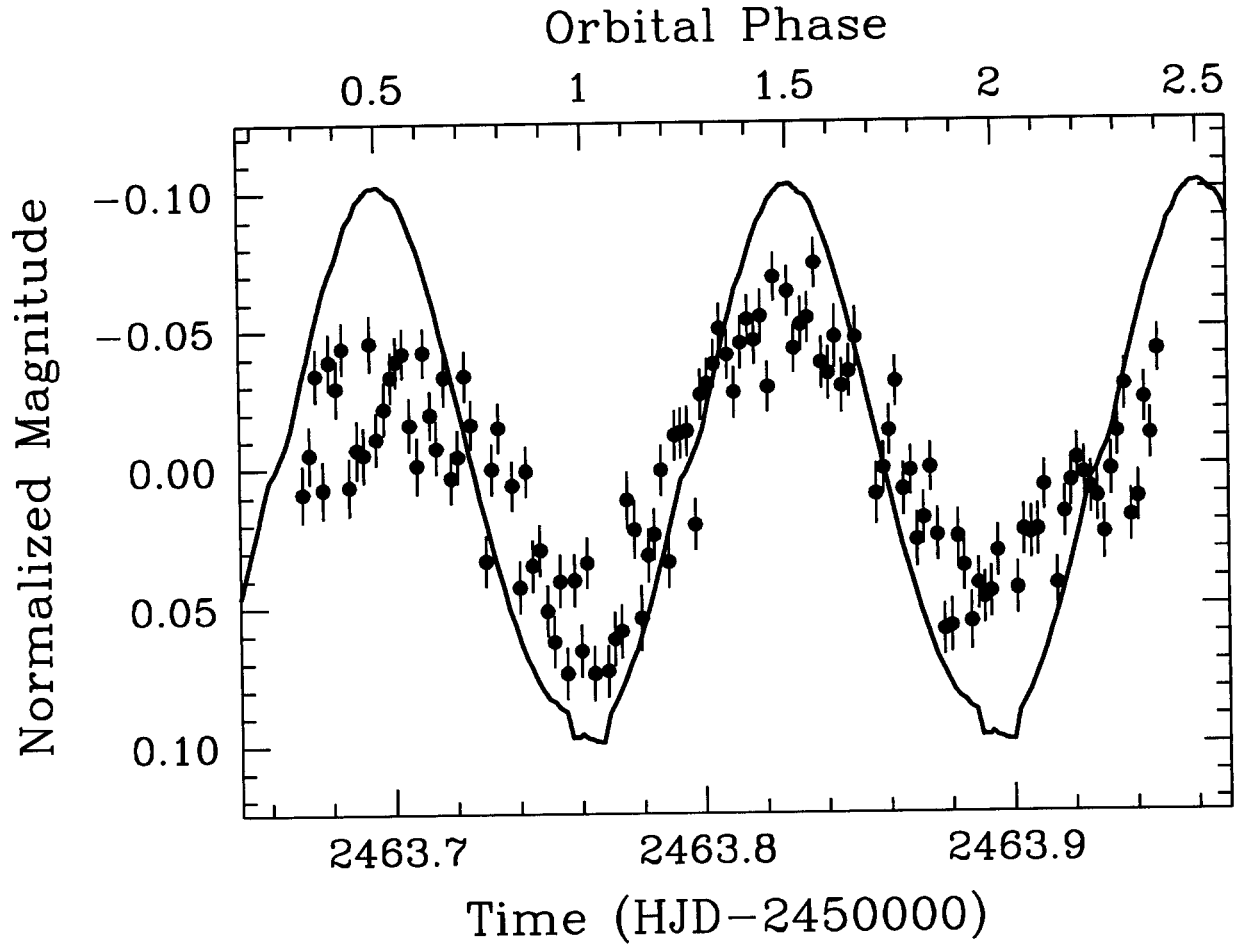


Fig. 7.— Optical light curve data of MV Lyr from Figure 2 (bottom panel) with the BINSYN model light curve (solid line) superposed. The mean magnitude of the observed data has been subtracted from the observed and model light curves.

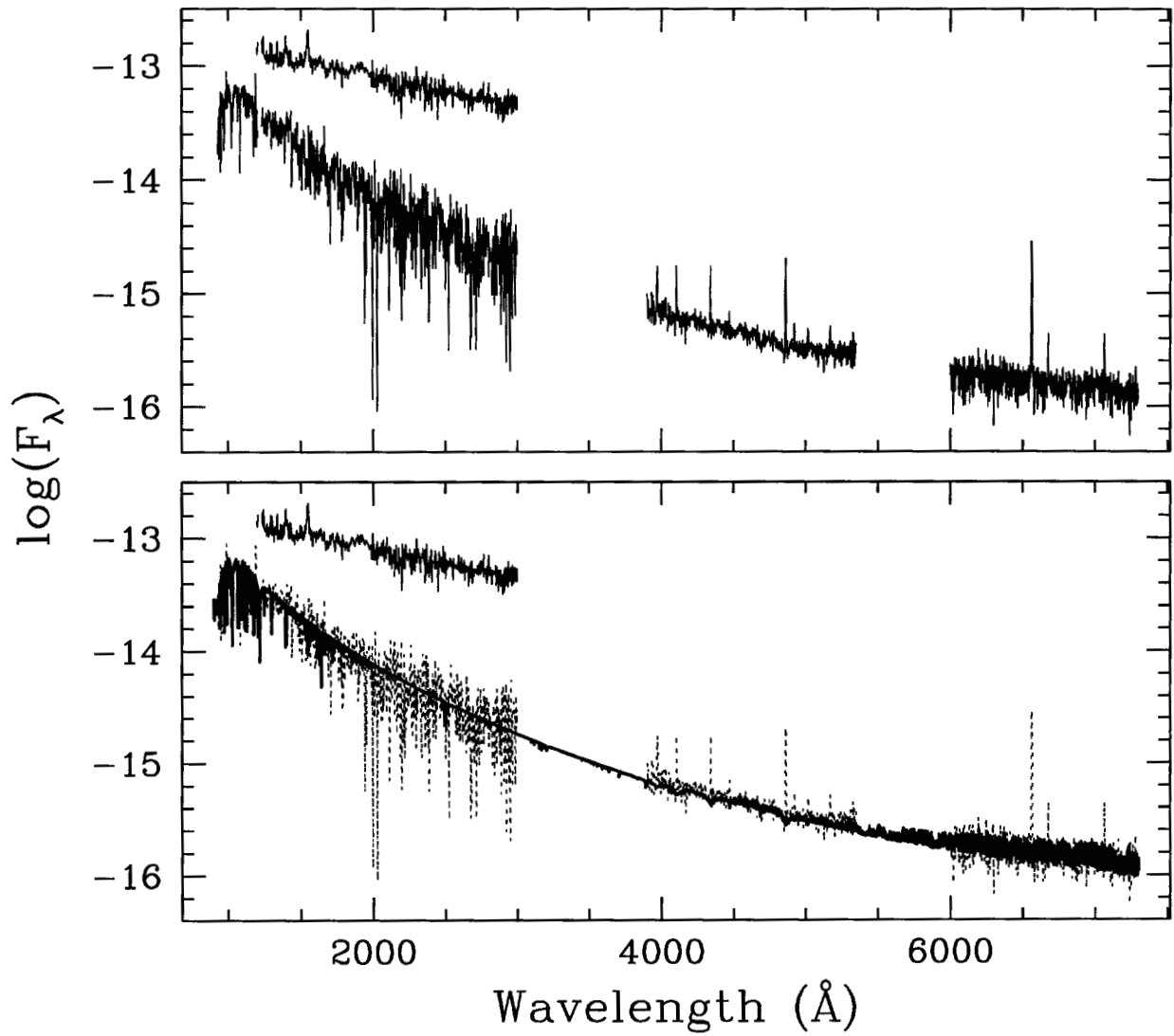


Fig. 8.— *FUSE*, *IUE*, and optical spectra of MV Lyr. Top panel shows the faint state spectra (lower data), as well as additional *IUE* spectra of MV Lyr obtained during the bright state (upper data), for comparison. Bottom panel shows the same spectra from the top panel with the BINSYN model spectrum (solid black line in print version; blue line in electronic version) superposed on the low state spectra (dotted line in print version; solid line in electronic version). The prominent geocoronal lines in the *FUSE* and *IUE* spectra have been masked off.